

Early-to-mid stage idiopathic Parkinson's disease shows enhanced cytotoxicity and differentiation in CD8 T-cells in females

Supplementary Information

Christophe M. Capelle^{1, 2, §}, Séverine Ciré^{1, £}, Fanny Hedin³, Maxime Hansen^{4, 5}, Lukas Pavelka^{4, 5, 6}, Kamil Grzyb⁴, Dimitrios Kyriakis^{4, ¥}, Oliver Hunewald¹, Maria Konstantinou³, Dominique Revets³, Vera Tslaf^{1, 2, 6}, Tainá M. Marques⁶, Clarissa P. C. Gomes⁴, Alexandre Baron¹, Olivia Domingues¹, Mario Gomez³, Ni Zeng^{1, 2}, Fay Betsou^{7, 8}, Patrick May⁴, Alexander Skupin^{4, 9, 10}, Antonio Cosma³, Rudi Balling^{4, 11}, Rejko Krüger^{4, 5, 6}, Markus Ollert^{1, 12, *}, Feng Q. Hefeng^{1, 13, *}

¹ Department of Infection and Immunity, Luxembourg Institute of Health (LIH), 29, rue Henri Koch, L-4354, Esch-sur-Alzette, Luxembourg

² Faculty of Science, Technology and Medicine, University of Luxembourg, 2, avenue de Université, L-4365, Esch-sur-Alzette, Luxembourg

³ National Cytometry Platform, Luxembourg Institute of Health, 29, rue Henri Koch, L-4354 Esch-sur-Alzette, Luxembourg

⁴ Luxembourg Centre for Systems Biomedicine (LCSB), University of Luxembourg, 6, avenue du Swing, L-4367, Belvaux, Luxembourg

⁵ Parkinson Research Clinic, Centre Hospitalier de Luxembourg (CHL), 4, Rue Nicolas Ernest Barblé, L-1210, Luxembourg, Luxembourg

⁶ Transversal Translational Medicine, Luxembourg Institute of Health, 1A-B, rue Thomas Edison, L-1445, Strassen, Luxembourg

⁷ Integrated Biobank of Luxembourg (IBBL), 1, rue Louis Rech, L-3555, Dudelange, Luxembourg

⁸ CRBIP, Institut Pasteur, Université Paris Cité, Paris, France

⁹ Department of Physics and Material Science, 162a, av. de la Faïencerie, L-1511, Luxembourg, Luxembourg

¹⁰ Department of Neurosciences, University California San Diego School of Medicine, 9500 Gilman Drive, La Jolla, CA 92093-0662, USA

¹¹ Institute of Molecular Psychiatry, University of Bonn, Venusberg-Campus 1, D-53127, Bonn, Germany

¹² Department of Dermatology and Allergy Center, Odense Research Center for Anaphylaxis (ORCA), University of Southern Denmark, Odense, 5000 C, Denmark

¹³ Data Integration and Analysis Unit, Luxembourg Institute of Health (LIH), L-1445 Strassen, Luxembourg

[§] Current address, Institute of Microbiology, ETH Zurich, Vladimir-Prelog-Weg 4, CH-8049 Zurich, Switzerland

[£] Current address, Eligo Bioscience, 111, avenue de France, 75013 Paris, France

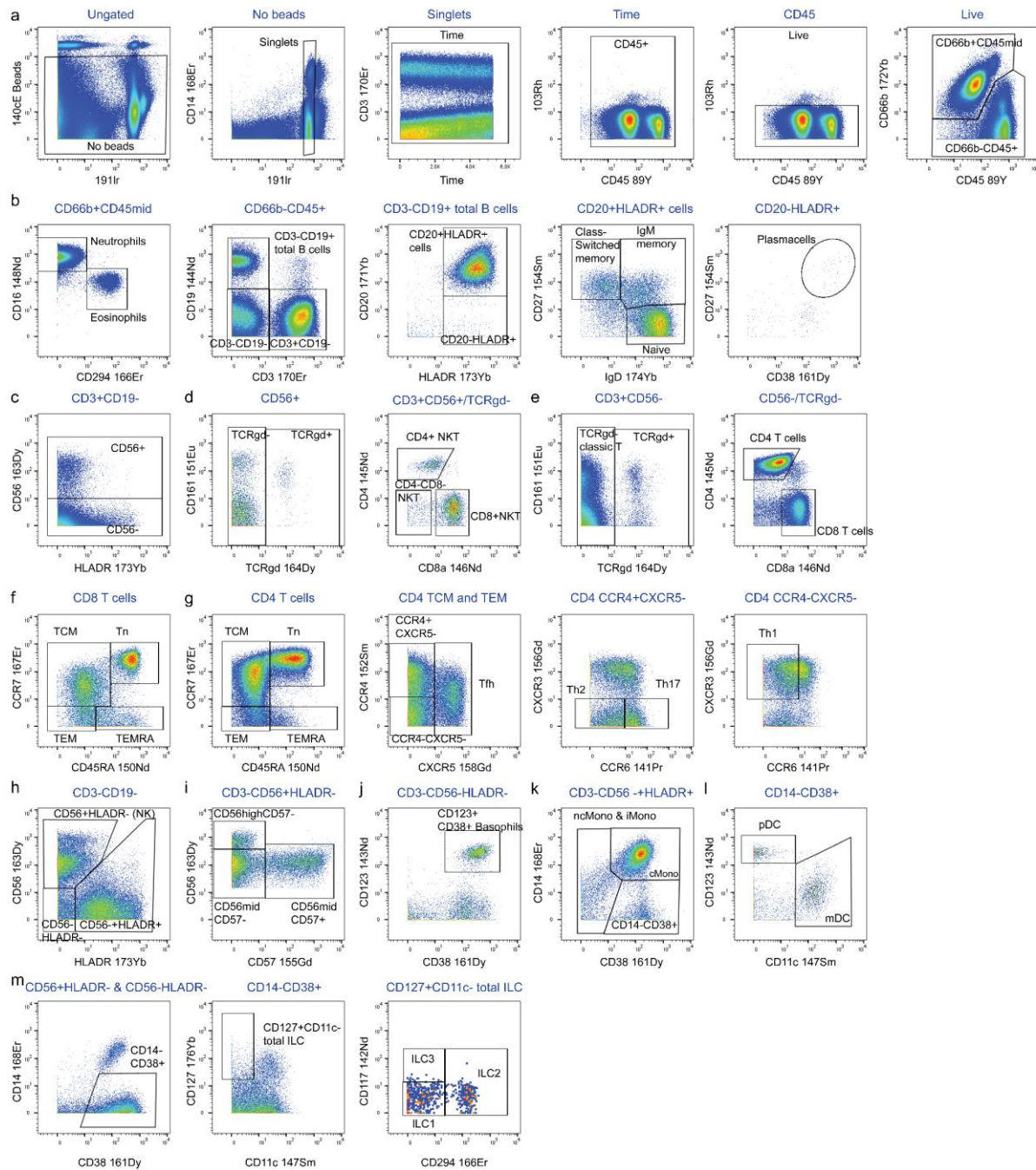
[¥] Current address, Icahn School of Medicine at Mount Sinai, New York, NY 10029, USA

* Corresponding author. Correspondence to M.O. (Markus.ollert@lih.lu) or F.Q.H. (feng.he@lih.lu)

Supplementary Note 1: Extended acknowledgement to the consortium members of the cohort used in this work.

We would like to thank all the anonymous participants of the Luxembourg Parkinson's Study for their important support of our research. Furthermore, we acknowledge the joint effort of the National Centre of Excellence in Research on Parkinson's Disease (NCER-PD) Consortium members from the partner institutions Luxembourg Centre for Systems Biomedicine, Luxembourg Institute of Health, Centre Hospitalier de Luxembourg, and Laboratoire National de Santé generally contributing to the Luxembourg Parkinson's Study as listed below: Geeta ACHARYA², Gloria AGUAYO², Myriam ALEXANDRE², Muhammad ALI¹, Wim AMMERLANN², Giuseppe ARENA¹, Rudi BALLING¹, Michele BASSIS¹, Roxane BATUTU³, Katy BEAUMONT², Regina BECKER¹, Camille BELLORA², Guy BERCHEM³, Daniela BERG¹¹, Alexandre BISSDORFF⁵, Ibrahim BOUSSAAD¹, Kathrin BROCKMANN¹¹, Jessica CALMES², Lorieza CASTILLO², Gessica CONTESOTTO², Nancy DE BREMAEKER³, Nico DIEDERICH³, Rene DONDELINGER⁵, Daniela ESTEVES², Guy FAGHERAZZI², Jean-Yves FERRAND², Manon GANTENBEIN², Thomas GASSER¹¹, Piotr GAWRON¹, Soumyabrata GHOSH¹, Marijus GIRAITIS^{2,3}, Enrico GLAAB¹, Elisa GÓMEZ DE LOPE¹, Jérôme GRAAS², Mariella GRAZIANO¹⁷, Valentin GROUES¹, Anne GRÜNEWALD¹, Wei GU¹, Gaël HAMMOT², Anne-Marie HANFF², Linda HANSEN^{1,3}, Michael HENEKA¹, Estelle HENRY², Sylvia HERBRINK⁶, Sascha HERZINGER¹, Michael HEYMANN², Michele HU⁸, Alexander HUNDT², Nadine JACOBY¹⁸, Jacek JAROSLAW LEBIODA¹, Yohan JAROZ¹, Sonja JÓNSDÓTTIR², Quentin KLOPFENSTEIN¹, Jochen KLUCKEN^{1,2,3}, Rejko KRÜGER^{1,2,3}, Pauline LAMBERT², Zied LANDOULSI¹, Roseline LENTZ⁷, Inga LIEPELT¹¹, Robert LISZKA¹⁴, Laura LONGHINO³, Victoria LORENTZ², Paula Cristina LUPU², Clare MACKAY¹⁰, Walter MAETZLER¹⁵, Katrin MARCUS¹³, Guilherme MARQUES², Tainá M. MARQUES¹, Patricia MARTINS CONDE¹, Patrick MAY¹, Deborah MCINTYRE², Chouaib MADIOUNI², Françoise MEISCH¹, Myriam MENSTER², Maura MINELLI², Michel MITTELBRONN^{1,4}, Brit MOLLENHAUER¹², Friedrich MÜHLSCHLEGEL⁴, Romain NATI³, Ulf NEHRBASS², Sarah NICKELS¹, Beatrice NICOLAI³, Jean-Paul NICOLAY¹⁹, Fozia NOOR², Marek OSTASZEWSKI¹, Clarissa P. C. GOMES¹, Sinthuja PACHCHEK¹, Claire PAULY^{1,3}, Laure PAULY¹, Lukas PAVELKA^{1,3}, Magali PERQUIN², Rosalina RAMOS LIMA², Armin RAUSCHENBERGER¹, Rajesh RAWAL¹, Dheeraj REDDY BOBBILI¹, Kirsten ROOMP¹, Eduardo ROSALES², Isabel ROSETY¹, Estelle SANDT², Stefano SAPIENZA¹, Venkata SATAGOPAM¹, Margaux SCHMITT², Sabine SCHMITZ¹, Reinhard SCHNEIDER¹, Jens SCHWAMBORN¹, Amir SHARIFY², Ekaterina SOBOLEVA¹, Kate SOKOLOWSKA², Hermann THIEN², Elodie THIRY³, Rebecca TING JIIN LOO¹, Christophe TREFOIS¹, Johanna TROUET², Olena TSURKALENKO², Michel VAILLANT², Mesele VALENTI², Carlos VEGA¹, Liliana VILAS BOAS³, Maharshi VYAS¹,

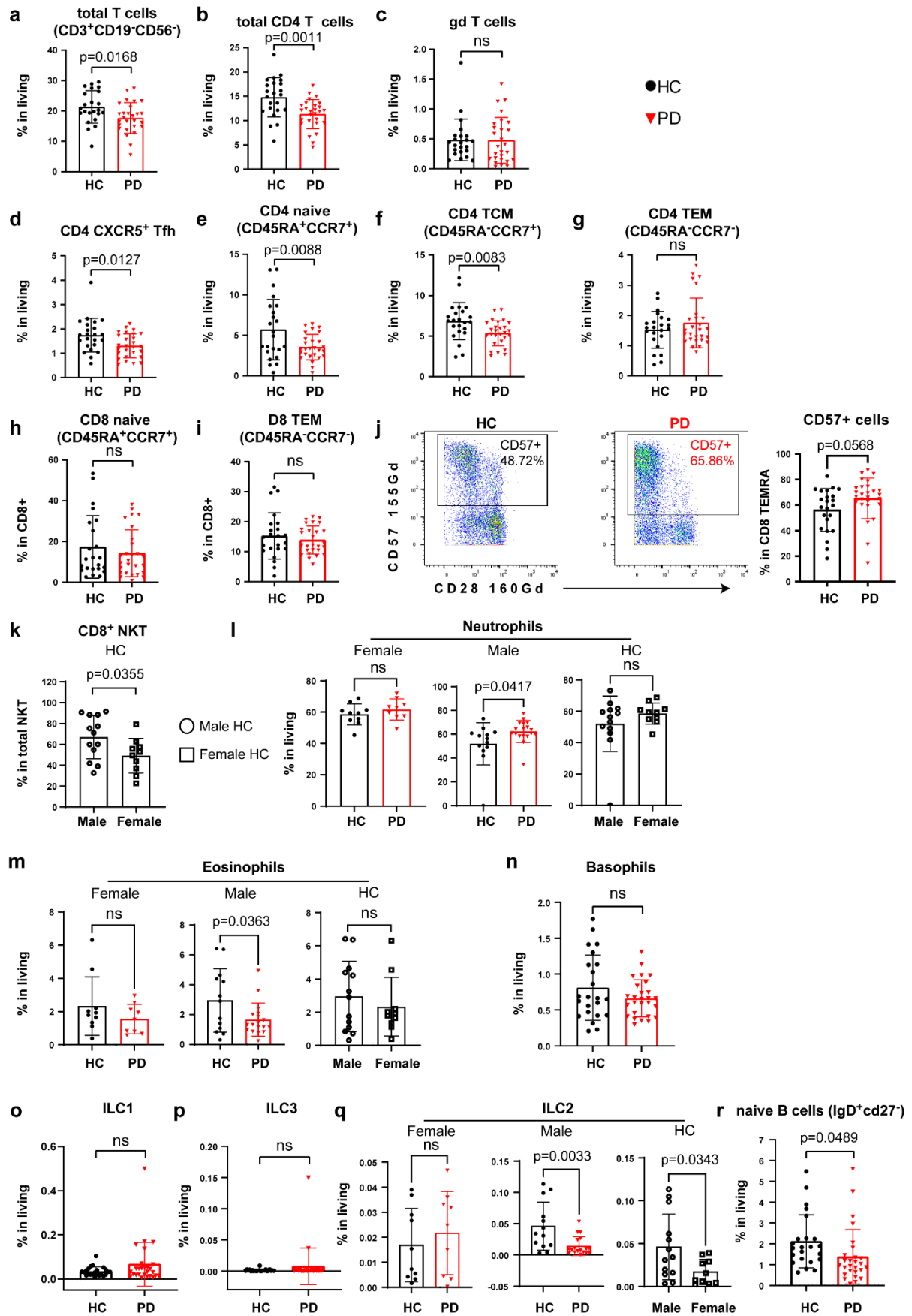
Richard WADE-MARTINS⁹, Paul WILMES¹, Evi WOLLSCHIED-LENGELING¹, Gelani ZELIMKHANOV³. The affiliations of individuals are listed as follows. ¹ Luxembourg Centre for Systems Biomedicine, University of Luxembourg, Esch-sur-Alzette, Luxembourg; ² Luxembourg Institute of Health, Strassen, Luxembourg; ³ Centre Hospitalier de Luxembourg, Strassen, Luxembourg; ⁴ Laboratoire National de Santé, Dudelange, Luxembourg; ⁵ Centre Hospitalier Emile Mayrisch, Esch-sur-Alzette, Luxembourg; ⁶ Centre Hospitalier du Nord, Ettelbrück, Luxembourg; ⁷ Parkinson Luxembourg Association, Leudelange, Luxembourg; ⁸ Oxford Parkinson's Disease Centre, Nuffield Department of Clinical Neurosciences, University of Oxford, Oxford, UK; ⁹ Oxford Parkinson's Disease Centre, Department of Physiology, Anatomy and Genetics, University of Oxford, Oxford, UK; ¹⁰ Oxford Centre for Human Brain Activity, Wellcome Centre for Integrative Neuroimaging, Department of Psychiatry, University of Oxford, Oxford, UK; ¹¹ Center of Neurology and Hertie Institute for Clinical Brain Research, Department of Neurodegenerative Diseases, University Hospital Tübingen, Tübingen, Germany; ¹² Paracelsus-Elena-Klinik, Kassel, Germany; ¹³ Ruhr-University of Bochum, Bochum, Germany; ¹⁴ Westpfalz-Klinikum GmbH, Kaiserslautern, Germany; ¹⁵ Department of Neurology, University Medical Center Schleswig-Holstein, Kiel, Germany; ¹⁶ Department of Neurology Philipps, University Marburg, Marburg, Germany; ¹⁷ Association of Physiotherapists in Parkinson's Disease Europe, Esch-sur-Alzette, Luxembourg; ¹⁸ Private practice, Ettelbruck, Luxembourg; ¹⁹ Private practice, Luxembourg, Luxembourg.



Supplementary Fig. 1. CyTOF gating strategy used in this study.

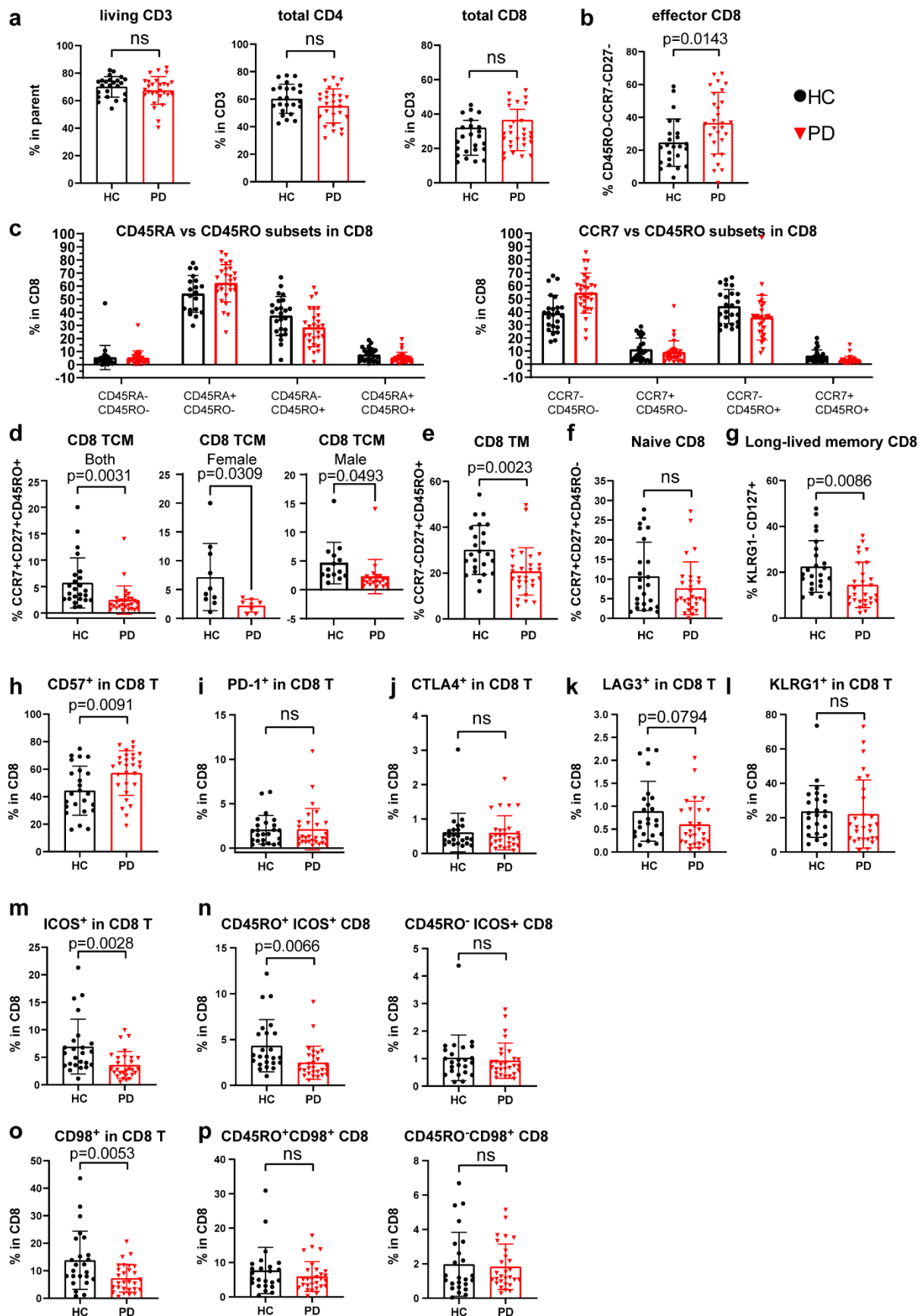
The gating strategy of the CyTOF analysis for various peripheral immune (sub-)populations from whole blood. The CyTOF markers used in this study are provided in **Supplementary Table 3**. Labels for some of the major subsets are enlarged. The corresponding parent gate was labelled in blue above the corresponding cytometry plot. To increase the explorability, we divided the overall gating strategy into different subpanels, including the initial general gating (singlet, living cells etc.) **(a)**, B cell subsets and neutrophils/eosinophils gates **(b)**, gates separating CD56+/CD56- cells **(c)**, natural killer T (NKT) subsets **(d)**, gdT cells as well as total CD4 and CD8 T cells **(e)**, CD8 naïve/memory subsets **(f)**, CD4 subsets **(g)**, natural killer (NK)

starting gates (**h**), NK subsets (**i**), basophils (**j**), monocyte subsets (**k**), dendritic cell (DC) subsets (**l**) and innate lymphoid cell (ILC) subsets (**m**). cMono, classical monocytes; iMono, intermediate monocytes; ncMono, non-classical monocytes; mDC, myeloid DC; pDC, plasmacytoid DC; Tn, naïve T cells; TCM, central memory T cells; TEM, effector memory T cells; TEMRA, terminally-differentiated effector memory T cells; Th1/Th2/Th17, type 1/2/17 T helper cells; Tfh, T follicular helper cells.



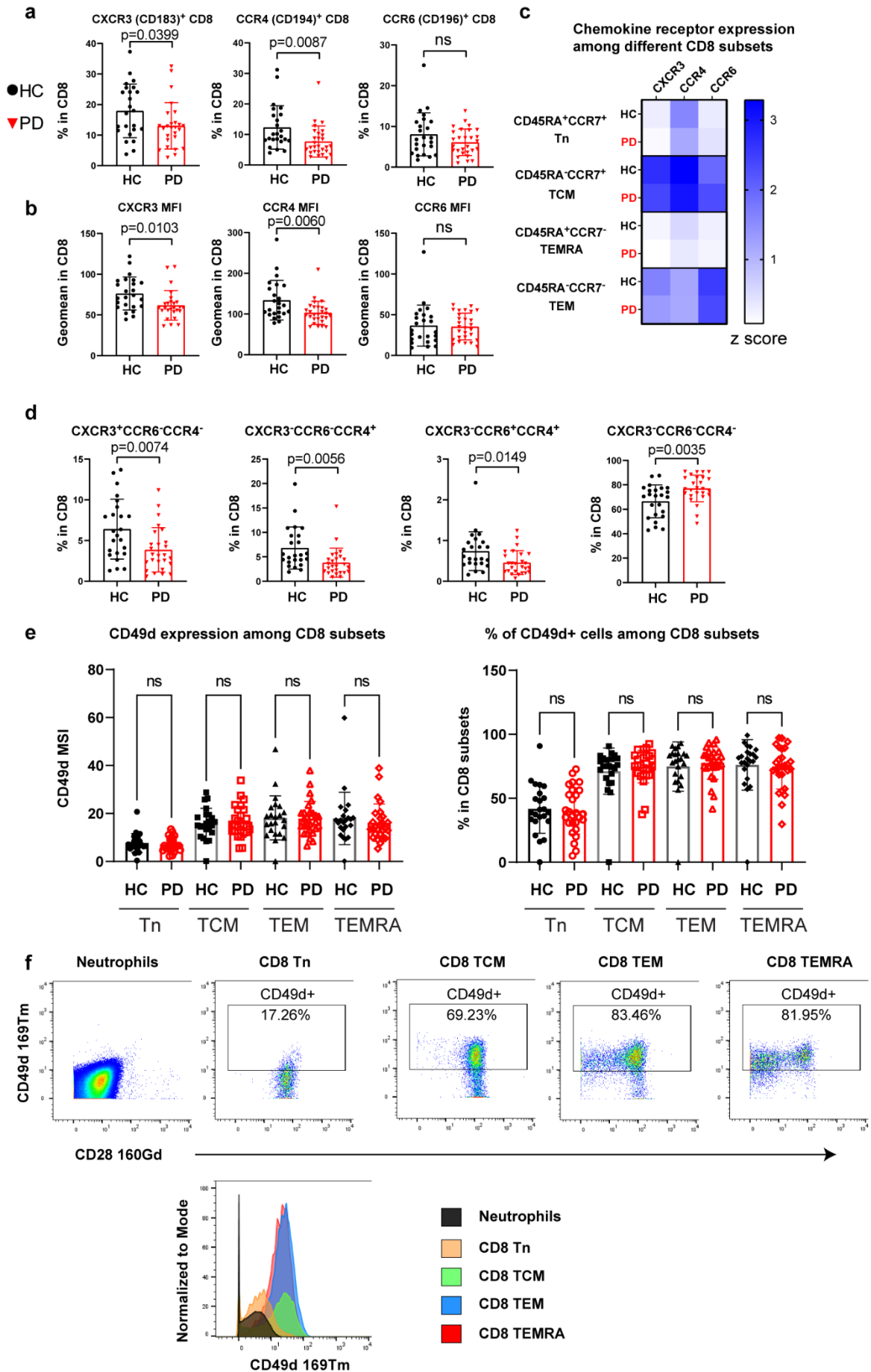
Supplementary Fig. 2. Extended analysis on major immune subsets examined by CyTOF.

a-c Scatter dot plots showing the frequency of total CD3 T cells (CD3⁺CD19⁻CD56⁻) (**a**), total CD4 T cells (**b**) and $\gamma\delta$ T cells (**c**) among living CD45⁺ cells in PD and HC, as analyzed by CyTOF. **d-g** Scatter dot plots showing the frequency of circulating CD4 CXCR5⁺ T follicular help (Tfh) (**d**), CD45RA⁺CCR7⁺ naïve (**e**), CD45RA⁻CCR7⁺ central memory (TCM) (**f**) and CD45RA⁻CCR7⁻ effector memory (TEM) (**g**) T cells. **h, i** Scatter dot plots showing the frequency of CD45RA⁺CCR7⁺ naïve (**h**) and CD45RA⁻CCR7⁻ effector memory (TEM) (**i**) among CD8 T cells. (**j**) Scatter dot plots showing the frequency of CD57⁺ cells among CD8 TEMRA (CD45RA⁺CCR7⁻). Left panel, representative cytometry plots showing the expression of CD57 and CD28 in CD8 TEMRA. **k** Scatter dot plots showing the frequency of CD8⁺ NKT among total NKT between male and female HC. **l, m, q** Scatter dot plots showing the frequency of neutrophils (**l**), eosinophils (**m**) or ILC2 (**q**) among living CD45⁺ singlets in female (left) or male (middle) participants. The comparison between female and male HC was displayed in the right subpanel. **n-p, r** Scatter dot plots showing the frequency of basophils (**n**), ILC1 (**o**), ILC3 (**p**) and naïve B cells (**r**) among living CD45⁺ immune cells. For detailed gating strategy, please refer to **Supplementary Fig. 1**. All the statistical description of major immune subsets was also provided in **Supplementary Table 5**. The combination of markers defining the corresponding subset was directly displayed in the panel title (**a-i**). The results were analyzed using unpaired two-tailed Student's *t* test. Data are presented as mean of the given group \pm standard deviation (s.d.). Each symbol represents the measurement from one individual participant (**a-r**). ns, not significant; all significant P-values are indicated. HC, healthy controls, n=24; PD, patients with Parkinson's disease, n=28. Of note, one PD and one HC were excluded due to technical failure during CyTOF staining. Female HC, n=10; female PD, n=9; male HC, n=13; male PD, n=18. NKT, Natural killer cells; ILC, innate lymphoid cells. Source data are provided as a Source Data file.



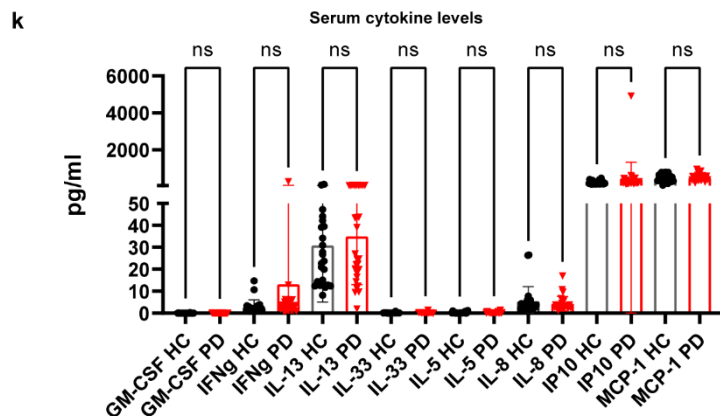
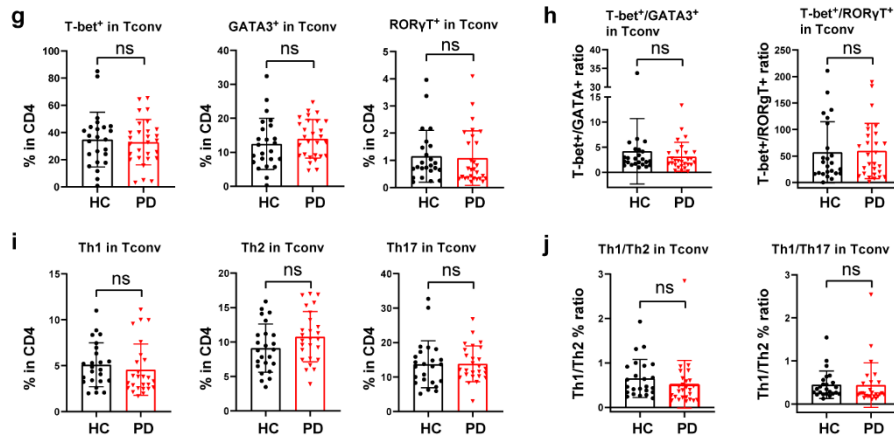
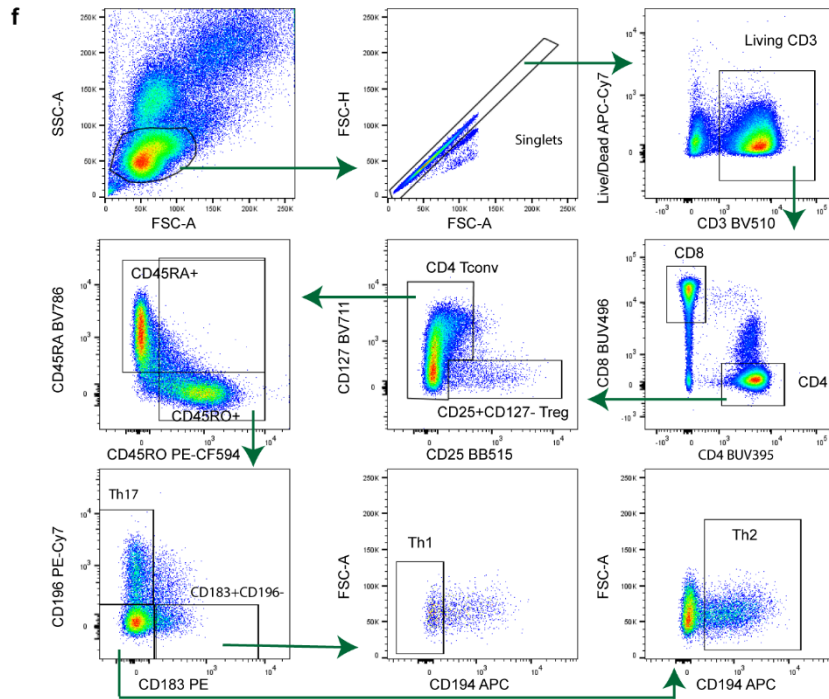
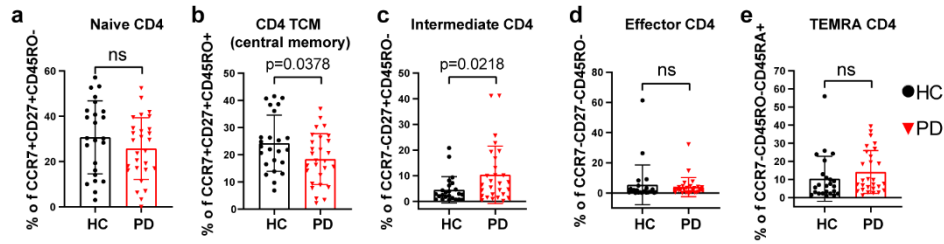
Supplementary Fig. 3. Early-to-mid stage iPD shows fewer memory CD8 T cells and displays no sign of accelerated exhaustion.

a Scatter dot plots showing the frequency of total CD3, CD4 and CD8 T cells in PD and HC as analyzed by FCM. The parent gate of CD3⁺ cells is living lymphocyte singlets. **b** Scatter dot plots showing the frequency of effector CD8 T cells among total CD8 T cells. **c** Scatter dot plots showing the proportions of CD45RA vs CD45RO (left) and CCR7 vs CD45RO (right) quartered subpopulations of CD8 T cells. **d-g** Scatter dot plots showing the frequency of TCM (central memory) (**d**) for all (left) or females (middle) or males (right), TM (transitional memory) (**e**), naïve (**f**) and long-lived memory (**g**) among CD8 T cells in PD and HC. The combination of markers defining the corresponding subset was directly labelled in the y-axis title. **h-l** Scatter dot plots showing the frequency of CD57⁺ (**h**), PD-1⁺ (**i**), CTLA4⁺ (**j**), LAG3⁺ (**k**) and KLRG1⁺ (**l**) populations among CD8 T cells. **m, n** Scatter dot plots showing the frequency of ICOS⁺ cells (**m**), ICOS⁺CD45RO⁺ or ICOS⁺CD45RO⁻ cells (**n**) among total CD8 T cells in PD and HC. **o, p** Scatter dot plots showing the frequency of total CD98⁺ populations (CD98: amino acid transporter) (**o**) as well as CD98⁺CD45RO⁺ or CD98⁺CD45RO⁻ cells (**p**) among total CD8 T cells. The results were analyzed using unpaired two-tailed Student *t* test. Data are presented as mean of the given group ± standard deviation (s.d.). Each symbol represents the measurement from one individual (**a-p**). ns, not significant; all significant P-values are indicated (except for **c**, where the purpose was only to show the relative average proportions of each of the four subsets). HC, healthy controls, n=24; PD, patients with Parkinson's disease, n=28. Female HC, n=10; female PD, n=8; male HC, n=14; male PD, n=19. Of note, for **d**, one female PD sample was excluded as the same patient visited twice within a short period. Source data are provided as a Source Data file.



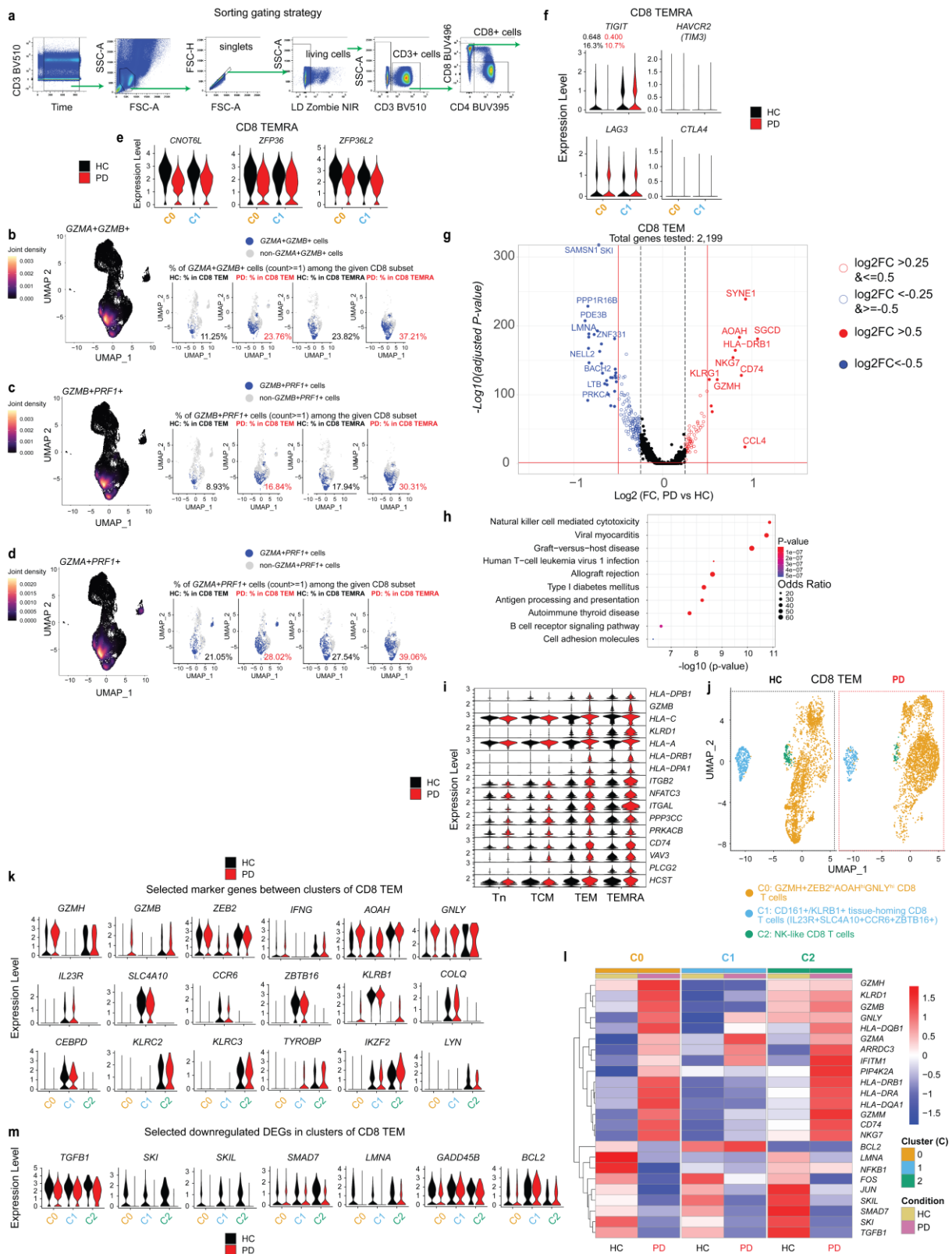
Supplementary Fig. 4. CD8 TEMRA show normal expression of analyzed chemokine receptors and CD49d in early-to-mid stage iPD.

a Scatter dot plots showing the frequency of CXCR3/CD183, CCR4/CD194 and CCR6/CD196 positive cells among total CD8 T cells. **b** Scatter dot plots showing the geometric mean (geomean, reflecting MFI) of CXCR3, CCR4 and CCR6 among total CD8 T cells. **c** Heatmap showing the averaged expression levels of the analyzed chemokine receptors in subpopulations of CD8 T cells for the given group. The frequency of cells expressing the given chemokine receptor was normalized along column. CCR7 expression was not shown because CCR7 was used to define CD8 naïve/memory T-cell subsets. **d** Scatter dot plots showing the frequency of CD8 T cells expressing different combinations of the chemokine receptors CXCR3, CCR4 and CCR6. **e** Scatter dot plots showing the expression level (MSI) of the brain homing factor CD49d (left) or the frequency of CD49d⁺ cells (right) among different CD8 T-cell subsets. **f** Representative cytometry plots showing the expression of CD49d and CD28 among different cell types. Neutrophils were used as the negative controls here as they are known to be largely CD49d⁻ in humans (Massena et al. 2015). Lower panel, histogram overlay of CD49d expression between different cell (sub) types. Data are presented as mean \pm standard deviation (s.d.). Each symbol represents the measurement from one individual participant (**a**, **b**, **d**, **e**). The results were analyzed using unpaired two-tailed Student's *t* test (**a**, **b**, **d**) while **e** was analyzed using ordinary one-way ANOVA test with two-stage linear step-up procedure of Benjamini/Krieger/Yekutieli correction. q-values (FDR) were analyzed for **e**. ns, not significant; all significant p-values are indicated. HC, healthy controls, n=24; PD, patients with Parkinson's disease, n=28; FCM, flow cytometry; MSI, median signal intensity; Tn, naïve T cells; TCM, central memory; TEM, effector memory. Of note, the CD49d expression was analyzed by CyTOF while the expression of the chemokine receptors was done using FCM. For FCM, two PD samples were excluded for CD183 related results where CD183 abs was missing during staining. Source data are provided as a Source Data file.



Supplementary Fig. 5. CD4 TCM frequency is reduced while the balance among CD4 T-helper subsets is unaffected in early-to-mid stage iPD.

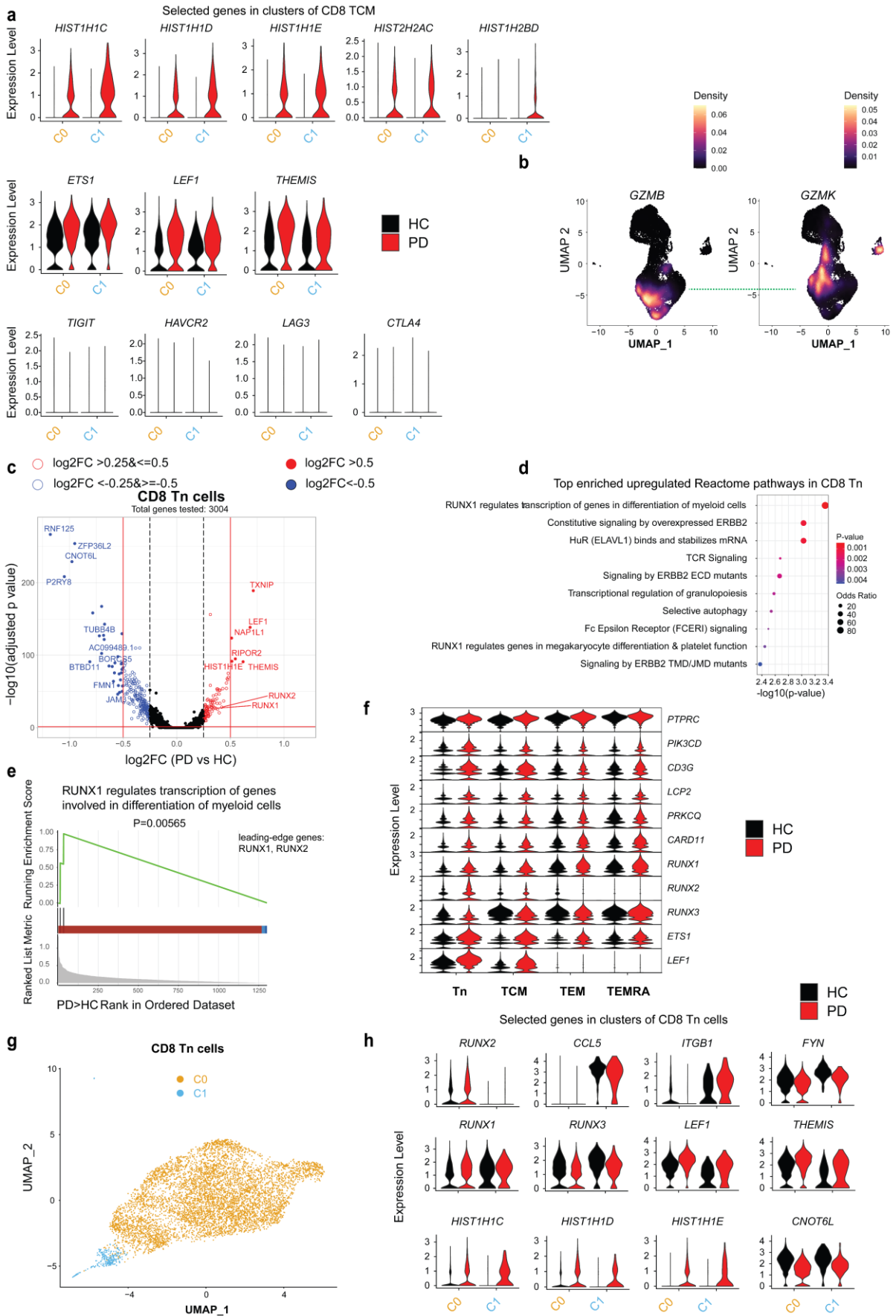
a-e Scatter dot plots showing the frequency of naïve (**a**), TCM (central memory) (**b**), intermediate (**c**), effector (**d**) and TEMRA (**e**) among CD4 T cells quantified by FCM. **f** Gating strategy to define CD4 Th1, Th2 and Th17 subsets based on the combinations of the expression of the chemokine receptors CXCR3/CD183, CCR4/CD194 and CCR6/CD196 using flow-cytometry analysis. Arrows indicate the gating workflow. **g** Scatter dot plots showing the expression of the master transcriptions factor (T-bet, GATA3 or ROR γ T) of CD4 T helper subset in PD and HC. **h** Ratios between T-bet⁺/GATA3⁺ and T-bet⁺/ROR γ T⁺ CD4 T cells in PD and HC, reflecting the ratios of Th1/Th2 and Th1/Th17, respectively. **i** Scatter dot plots showing the frequency of Th1 (CXCR3⁺CCR6⁻CCR4⁻), Th2 (CXCR3⁻CCR6⁻CCR4⁺) and Th17 (CXCR3⁻CCR6⁺) cells based on the combinations of the expression of the chemokine receptors CXCR3, CCR4 and CCR6. **j** Ratios of Th1/Th2 and Th1/Th17 cells in PD and HC. The ratios in **j** were calculated based on data of **i**. **k** Serological levels of other analysed cytokines/chemokines (except for those shown in **Fig. 2**) in PD and HC. Some values of the participants were excluded for certain cytokines because one technical replicate was detected while another replicate was below detection range or below fit curve range. The results were analysed using unpaired two-tailed Student's *t* test (**a-e**, **g-j**) or using Brown-Forsythe and Welch ANOVA test with Dunnett's T3 multiple comparison test (**k**). Data are presented as mean \pm standard deviation (s.d.). Each symbol represents the measurement from one individual (**a-e**, **g-j**, **k**). ns, not significant; all significant P-values are indicated. HC, healthy controls, n=24; PD, patients with Parkinson's disease, n=28; FCM, flow cytometry. Of note (**i**, **j**), two PD samples were excluded for CD183-related results where CD183 abs was missing during staining. Source data are provided as a Source Data file.



Supplementary Fig. 6. Cytotoxicity pathways are also enhanced in CD8 TEM of early-to-mid stage iPD as revealed by scRNA-seq.

a Gating strategy to sort four CD8 subsets (the last step in Fig. 6A). **b-d** UMAP (left) showing joint density of GZMA and GZMB (**b**), of GZMB and PRF1 (**c**) and of GZMA and PRF1 (**d**)

among all the CD8 T cells. Right, UMAP showing the cells co-expressing the indicated markers. For visual comparability, random downsampling was employed to display the same number of cells between different conditions and subsets. **e, f** Violin plots of selected downregulated (**e**) or exhaustion (**f**) markers in different clusters of CD8 TEMRA. The numbers under *TIGIT* indicate either the percentage of the cells expressing *TIGIT* (count \geq 1) or the average *TIGIT* expression in CD8 TEMRA of either PD (red) or HC (black) for Cluster 0 (C0). **g** Volcano plot showing the expression changes in CD8 TEM. The selected top up- or down-regulated genes (ranked based on gene score) were marked in red or blue labels, respectively. Vertical red solid lines indicates the log₂FC value of 0.5 and -0.5, respectively, while the horizontal red line indicates $-\log_{10}(0.05)$. **h** Top enriched KEGG pathways among upregulated genes in iPD vs HC in CD8 TEM. **i** Violin plots of selected DEGs involved in the top-enriched KEGG pathways (from **h**). **j** UMAP showing the unsupervised clustering analysis of CD8 TEM from iPD vs HC. For visual comparability, CD8 TEM cells were randomly downsampled to the same number between groups. **k, m** Violin plots of selected markers distinguishing different clusters (**k**) or selected iPD down-regulated genes (**m**) within CD8 TEM. **l** Heatmap of the selected most up- or down-regulated DEGs across different clusters in CD8 TEM of iPD vs HC. P-values in **g** and **h** were analyzed using two-tailed non-parametric Wilcoxon Rank test adjusted based on Bonferroni correction and the one-tailed Fisher's exact test, respectively. The genes selected in **k-m** were analyzed using two-tailed non-parametric Wilcoxon Rank test adjusted based on Bonferroni correction (only those with an adjusted P-value \leq 0.05 were considered). DEG, differentially-expressed genes; FC, fold change; UMAP, uniform manifold approximation and projection.



Supplementary Fig. 7. Transcriptionally-reprogramming already occurs in CD8 Tn of early-to-mid stage iPD.

a Violin plots of selected top DEGs or exhaustion marker genes in clusters of CD8 TCM. **b** UMAP showing the density of *GZMB* or *GZMK* expression in all the individual CD8 T cells analyzed by scRNA-seq. A dashed green line highlights the boundary between major *GZMB*- and *GZMK*-expressing zones. **c** Volcano plot showing the gene expression of CD8 Tn in iPD vs HC. The selected top up- or down-regulated genes (ranked based on gene score) were marked in red or blue labels, respectively. *RUNX1* and *RUNX2* were additionally labelled. Vertical red line indicates the log₂FC value of 0.5 or -0.5 while the horizontal red line indicates $-\log_{10}(0.05)$. **d** Top-ranked enriched Reactome pathways among up-regulated genes in CD8 Tn of iPD vs HC. **e** GSEA plot of the pathway showing the *RUNX1* transcription regulation involved in myeloid cell differentiation. The lower part showing the rank distribution of the genes involved in the indicated pathway. The list on the right showing the leading-edge genes. **f** Violin plots showing the genes involved in TCR signaling or early differentiation of CD8 T cells. **g** UMAP plot showing the unsupervised clustering analysis of CD8 Tn. **h** Violin plots of either selected genes distinguishing clusters or selected DEGs in iPD vs HC. P-values in **c** and **h** were analyzed using two-tailed non-parametric Wilcoxon Rank Sum test adjusted based on Bonferroni correction. In **h**, only those with an adjusted P-value ≤ 0.05 were included. P-values in **d** and **e** were analyzed using the one-tailed Fisher's exact test and the empirical phenotype-based permutation test, respectively. Each dot represents one single cell in **b**, **g**. DEG, differentially-expressed genes; FC, fold change; UMAP, uniform manifold approximation and projection.

Supplementary Table 1. The exclusion criteria of the cohort.

Exclusion Criteria	
History or presence of medication taken	Corticosteroids Cytostatic drugs Immunosuppressive treatment Iodine*
Medical history	Acute Infection Autoimmune Disorders Chronic Infections Endocrine Diseases Gastrointestinal Diseases Haematological Diseases

	Immunodeficiency Malignancies Neurologic Diseases (other than Parkinson's disease)
--	--

* Iodine treatment could interfere with the mass cytometry (CyTOF) staining and thus was also excluded.

Supplementary Table 2. Basic demographics and clinical information of the participants in various sub-cohorts analysed in this work.

Initial discovery cohort (fresh sampling)			
	PD (n=28)	HC (n=24)	P-value
Male, % (n)	68 (19)	58 (14)	0.477 (two-tailed Chi square test)
Age at sampling in years, mean (SD) [£]	64.9 (6.97)	63.92 (3.75)	0.54 (two-tailed Student <i>t</i> test)
Age of Onset, mean (SD)	58.14 (9.42)	NA	NA
Disease duration from diagnosis (years), mean (SD)	6.64 (4.12)	NA	NA
Disease duration from initial symptom onset, mean (SD)	8.19 (5.37)	NA	NA
Family History of Parkinson's Disease, % (n)	43 (12)	NA	NA
Hoehn and Yahr (H&Y) Staging scale, mean (SD)	2.3 (0.42)	NA	NA
UPDRS-III*, mean (SD)	39.69 (13.15)	NA	NA
LEDD [‡] , mean (SD)	610.58 (344.06)	NA	NA
MOCA [€] , mean (SD)	25.21 (3.82)	NA	NA
Validation cohort (cryopreserved PBMC; all iPD)			
Male, % (n)	73 (8 out of 11)	58 (5 out of 12)	0.133 (two-tailed Chi square test)
Age at sampling, mean (SD)	64.90 (3.96)	63.46 (3.72)	0.38 (two-tailed Student <i>t</i> test)
Age of Onset, mean (SD)	59.08 (5.54)	NA	NA
Disease duration from diagnosis (years), mean (SD)	4.45 (3.21)	NA	NA
Disease duration from initial symptom onset, mean (SD)	5.82 (3.89)	NA	NA
Hoehn and Yahr (H&Y) Staging scale, mean (SD)	2.0 (0.27)	NA	NA
Participants for scRNA-seq (cryopreserved PBMC; all iPD)			
Female,% (n)	100 (5)	100 (4)	NA (two-tailed Chi square test)
Age at sampling, mean (SD)	63.14 (4.08)	62.33 (2.68)	0.77 (two-tailed Student <i>t</i> test)
Age of Onset, mean (SD)	54.34 (9.17)	NA	NA
Disease duration from diagnosis (years), mean (SD)	6.4 (7.40)	NA	NA
Disease duration from initial symptom onset, mean (SD)	8.8 (9.55)	NA	NA
Hoehn and Yahr (H&Y) Staging scale, mean (SD)	All with 2.0	NA	NA

£descriptive statistics here includes information from all idiopathic and three genetic PD.

*UPDRS-III: Motor Examination. The physician does a number of tests to rate the cardinal symptoms of PD such as rigidity, postural instability, facial expression etc.

¥LEDD: Levodopa Equivalent Daily Dose, so basically the sum of levodopa a patient is taking each day.

€MOCA: Montreal Cognitive Assessment. Provides an overall cognitive profile (0-30, with 30 meaning no cognitive deficits).

NA, no data available or not applicable; SD, standard deviation.

Supplementary Table 3. List of CyTOF antibodies (Abs) used to stain the whole blood.

Metal Isotope	Antibody	Clone	Manufacturer	Catalogue#
89Y	CD45	HI30	Fluidigm	Part of MDIPA (201325)
103Rh	Live/Dead indicator		Fluidigm	Part of MDIPA
141Pr	CD196 (CCR6)	G034E3	Fluidigm	Part of MDIPA
142Nd	CD117 (c-kit)*	104D2	Biolegend	313223
143Nd	CD123	6H6	Fluidigm	Part of MDIPA
144Nd	CD19	HIB19	Fluidigm	Part of MDIPA
145Nd	CD4	RPA-T4	Fluidigm	Part of MDIPA
146Nd	CD8a	RPA-T8	Fluidigm	Part of MDIPA
147Sm	CD11c	Bu15	Fluidigm	Part of MDIPA
148Nd	CD16	3G8	Fluidigm	Part of MDIPA
149Sm	CD45RO	UCHL1	Fluidigm	Part of MDIPA
150Nd	CD45RA	HI100	Fluidigm	Part of MDIPA
151Eu	CD161	HP-3G10	Fluidigm	Part of MDIPA
152Sm	CD194 (CCR4)	L291H4	Fluidigm	Part of MDIPA
153Eu	CD25	BC96	Fluidigm	Part of MDIPA
154Sm	CD27	O323	Fluidigm	Part of MDIPA
155Gd	CD57	HCD57	Fluidigm	Part of MDIPA
156Gd	CD183 (CXCR3)	G025H7	Fluidigm	Part of MDIPA
158Gd	CD185 (CXCR5)	J252D4	Fluidigm	Part of MDIPA
159Tb	KLRG1*	SA231A2	Biolegend	367702
160Gd	CD28	CD28.2	Fluidigm	Part of MDIPA
161Dy	CD38	HB-7	Fluidigm	Part of MDIPA
162Dy	CD336 (NKP44)*	P44-8	Biolegend	325102
163Dy	CD56 (NCAM)	NCAM16.2	Fluidigm	Part of MDIPA
164Dy	TCRγδ	B1	Fluidigm	Part of MDIPA
165Ho	CD223 (LAG3)	11C3C65	Fluidigm	3165037B
166Er	CD294	BM16	Fluidigm	Part of MDIPA
167Er	CD197 (CCR7)	G043H7	Fluidigm	Part of MDIPA

168Er	CD14	63D3	Fluidigm	Part of MDIPA
169Tm	CD49d*	9F10	Biolegend	304302
170Er	CD3	UCHT1	Fluidigm	Part of MDIPA
171Yb	CD20	2H7	Fluidigm	Part of MDIPA
172Yb	CD66b	G10F5	Fluidigm	Part of MDIPA
173Yb	HLA-DR	LN3	Fluidigm	Part of MDIPA
174Yb	IgD	IA6-2	Fluidigm	Part of MDIPA
175Lu	CD279 (PD-1)	EH12.2H7	Fluidigm	3175008B
176Yb	CD127	A019D5	Fluidigm	Part of MDIPA

* in-house conjugation using Maxpar X8 Antibody Labeling Kits MDIPA (201325, Fluidigm). The predicted theoretical quantity (ug) used per reaction for the in-house conjugated Abs CD117-142Nd, KLRG1-159Tb, NKP44-162Dy, CD49d-169Tm, PD-1-175Lu and LAG3-165Ho was 0.5, 0.17, 0.5, 0.05, 0.17 and 0.05, respectively. The theoretical concentration was estimated based on the expected average recovery rate of 60% for an antibody conjugation procedure.

Supplementary Table 4. List of flow cytometry (FCM) Abs used to stain the PBMCs in this study.

Ab Target	Fluorochrome	Dilution	Manufacturer	Reference	Clone
Fc Blocking Abs	/	1:50	BD	564765	Fc1
CD3*	BUV737	1:100	BD	741822	HIT3a
CD3*	BV510	1:100	BD	564713	HIT3a
CD4	BUV395	1:100	BD	563550	SK3
CD8	BUV496	1:100	BD	564804	RPA-T8
CD25	BV786	1:50	BD	741035	2A3
CD25	BB515	1:50	BD	564467	2A3
CD27	BB700	1:50	BD	566450	M-T271
CD28	BUV785	1:50	BioLegend	302950	CD28.2
CD31	BV605	1:50	BD	562855	WM59
CD39	BV711	1:50	BioLegend	328228	A1
CD45RA	BV421	1:50	BioLegend	304130	HI100
CD45RA	BV785	1:50	BioLegend	304140	HI100

CD45RO	PE-CF594	1:50	BD	562299	UCHL1
CD57	FITC	1:50	BD	555619	NK-1
CD71	FITC	1:50	BioLegend	334104	CY1G4
CD98	BV786	1:50	BD	744507	UM7F8
CD122	PE	1:50	BioLegend	339006	TU27
CD127 (IL7R)	BV421	1:50	BD	562436	HIL-7R-M21
CD127 (IL7R)	BV711	1:50	BioLegend	351328	A019D5
CD183 (CXCR3)	PE	1:50	BD	560928	1C6/CXCR3
CD194 (CCR4)	APC	1:50	BioLegend	359408	L291H4
CD196 (CCR6)	PE-Cy7	1:50	BD	560620	11A9
CD197 (CCR7)	BV421	1:50	BioLegend	353208	G043H7
CD223 (LAG3)	BV711	1:50	BioLegend	369320	11C3C65
CD278 (ICOS)	BV605	1:50	BioLegend	313538	C398.4A
CD279 (PD-1)	BV605	1:50	BioLegend	329924	EH12.2H7
GLUT1 (SLC2A1)	PE	1:500	Abcam	ab209449	EPR3915
KLRG1	PE-Cy7	1:50	BioLegend	368614	14C2A07
Intracellular markers					
CD152 (CTLA4)	PE-Cy5	1:20	BD	555854	BNI3
FOXP3	APC	1:20	BioLegend	320114	206D
Phospho S6	AF488	1:20	CST	4803S	D57.2.2E
Helios	Pacific Blue	1:20	BioLegend	137220	22F6
Ki-67	Alex488	1:20	BD	561165	B56
GATA3	PE-Cy7	1:20	BD	560405	L50-823
RORγT	BV650	1:20	BD	563424	Q21-559
T-bet	PE	1:20	BioLegend	644810	4B10
Eomes	PE-Cy7	1:20	Thermo Fisher Scientific	25-4877-42	WD1928

Live/Dead	APC-Cy7	1:500	Thermo Fisher Scientific	L34976	/
-----------	---------	-------	--------------------------	--------	---

*, different fluorochromes of the same markers might be used in different staining panels as we simultaneously employed five staining panels to explore.

Supplementary Table 5. CyTOF analysis reveals the percentages of major immune subsets among living CD45+ singlets or among the relevant parent gates in the peripheral fresh blood of early-to-mid stage iPD or matched HC aged 60-70 years.

No.	Items	HC (n=24), mean (SD)	PD (n=28), Mean (SD)	P-value (two-tailed t test)
	Total number of living CD45+ singlets	627629 (136842)	679999 (155232)	0.22482
Among living CD45+ singlets				
1	ncMono plus interm Mono among living cells	0.847 (0.518)	0.75 (0.422)	0.476922
2	mDC among living cells	0.253 (0.065)	0.215 (0.07)	0.062098
3	pDC among living cells	0.111 (0.04)	0.097 (0.04)	0.24072
4	cMono among living cells	5.964 (1.085)	5.913 (1.37)	0.887997
5	Basophils among living cells	0.81 (0.445)	0.662 (0.253)	0.154289
6	NK among living cells	3.658 (1.6)	3.53 (1.747)	0.794596
7	CD56 ^{high} CD57 ⁻ immature NK among living cells	0.224 (0.131)	0.16 (0.088)	0.04992
8	CD56 ^{mid} CD57 ⁻ NK among living cells	1.619 (0.78)	1.549 (0.989)	0.788334
9	CD56 ^{mid} CD57 ⁺ late NK among living cells	1.815 (1.174)	1.823 (1.181)	0.982319
10	Total ILCs among living cells	0.069 (0.042)	0.091 (0.127)	0.419163
11	ILC1 among living cells	0.034 (0.021)	0.067 (0.098)	0.123848
12	ILC2 among living cells	0.033 (0.033)	0.017 (0.015)	0.025059
13	ILC3 among living cells	0.001 (0.002)	0.008 (0.029)	0.290684
14	B cells among living cells	3.24 (1.419)	3.453 (3.736)	0.801529
15	CD27 ⁺ CD38 ⁺ plasma cells among living cells	0.02 (0.021)	0.015 (0.01)	0.313471
16	CD20 ⁻ HLADR ⁺ among living cells	0.12 (0.37)	0.62 (2.09)	0.270256
17	CD20 ⁺ HLADR ⁺ among living cells	3.082 (1.363)	2.731 (3.217)	0.635057
18	CD27 ⁻ IgD ⁺ naïve B cells among living cells	2.12 (1.25)	1.379 (1.282)	0.04885
19	CD27 ⁺ IgD ⁻ class-switched memory B among living cells	0.395 (0.226)	0.385 (0.368)	0.911043

20	CD27 ⁺ IgD ⁺ IgM memory among living cells	0.39 (0.253)	0.781 (2.146)	0.39954
21	Total T cells among living cells	21.318 (5.235)	17.673 (4.946)	0.016814
22	TCRgd ⁺ classic T cells among living cells	20.835 (5.119)	17.198 (4.728)	0.013785
23	CD8 ⁺ T among living cells	5.42 (2.514)	5.372 (2.671)	0.950139
24	CD45RA ⁻ CCR7 ⁻ CD8 TEM among living cells	0.795 (0.453)	0.748 (0.43)	0.712639
25	CD45RA ⁻ CCR7 ⁺ CD8 CM among living cells	1.528 (0.963)	0.955 (0.536)	0.012486
26	CD45RA ⁺ CCR7 ⁻ CD8 TEMRA among living cells	2.165 (1.829)	2.839 (2.109)	0.247063
27	CD45RA ⁺ CCR7 ⁺ CD8 naïve T among living cells	0.783 (0.567)	0.72 (0.613)	0.713217
28	CD4 ⁺ among living cells	14.776 (3.947)	11.321 (2.945)	0.001126
29	CD45RA ⁻ CD4 among living cells	8.371 (2.389)	7.099 (1.927)	0.046814
30	CD4 CXCR3 ⁺ CCR6 ⁻ CCR4 ⁻ CXCR5 ⁻ Th1 among living cells	1.829 (0.745)	1.636 (0.958)	0.443708
31	CD4 CXCR3 ⁻ CCR6 ⁻ CCR4 ⁺ CXCR5 ⁻ Th2 among living cells	1.246 (0.535)	1.01 (0.41)	0.090831
32	CD4 CXCR3 ⁻ CCR6 ⁺ CCR4 ⁺ CXCR5 ⁻ Th17 among living cells	0.519 (0.319)	0.549 (0.329)	0.749899
33	CD4 CXCR5 ⁺ Tfh among living cells	1.741 (0.678)	1.304 (0.485)	0.012681
34	CD45RA ⁻ CCR7 ⁻ CD4 T among living cells	1.527 (0.594)	1.756 (0.81)	0.276958
35	CD45RA ⁻ CCR7 ⁺ CD4 T among living cells	6.848 (2.238)	5.345 (1.518)	0.008301
36	CD45RA ⁺ CCR7 ⁻ CD4 T among living cells	0.547 (0.598)	0.566 (0.647)	0.91715
37	CD45RA ⁺ CCR7 ⁺ CD4 T among living cells	5.699 (3.643)	3.55 (1.543)	0.00885
38	TCRgd ⁺ T among living cells	0.483 (0.341)	0.475 (0.376)	0.943847
39	NKT among living cells	2.407 (2.604)	2.431 (1.738)	0.969286
40	CD8 ⁺ NKT among living cells	1.33 (1.146)	1.722 (1.345)	0.287332
41	CD4 ⁺ NKT among living cells	0.973 (1.737)	0.546 (0.869)	0.27652
42	Eosinophils among living cells	2.682 (1.914)	1.628 (1.005)	0.018555
43	Neutrophils among living cells	54.853 (13.872)	62.153 (8.156)	0.028426
Among parent gate				
44	ncMono plus interm Mono among CD3 ⁻ CD19 ⁻ CD56 ⁻ HLADR ⁺	11.35 (5.243)	10.469 (4.895)	0.550335
45	cDC among CD14 ⁻ CD38 ⁺	58.174 (5.712)	56.277 (9.996)	0.434193
46	pDC among CD14 ⁻ CD38 ⁺	25.269 (6.242)	25.391 (8.386)	0.955228
47	cMono among CD56 ⁺ HLADR ⁺	82.436 (5.429)	83.938 (5.407)	0.343294
48	Basophils among CD56 ⁻ HLADR ⁻	58.465 (18.293)	55.279 (15.374)	0.515111

49	NK among CD3 ⁻ CD19 ⁻	28.807 (8.605)	28.745 (10.793)	0.982812
50	CD56 ^{high} CD57 ⁻ immature NK among NK	7.04 (4.954)	6.009 (5.045)	0.47997
51	CD56 ^{mid} CD57 ⁻ among NK	46.359 (13.894)	43.532 (15.477)	0.511909
52	CD56 ^{mid} CD57 ⁺ late NK among NK	46.593 (16.195)	50.501 (16.552)	0.414395
53	Total ILCs among CD14 ⁻ CD38 ⁺	1.831 (1.191)	2.776 (3.886)	0.276966
54	ILC1 among ILCs	56.917 (22.262)	67.578 (21.7)	0.100179
55	ILC2 among ILCs	40.648 (23.368)	28.852 (22.595)	0.082335
56	ILC3 among ILCs	2.447 (3.122)	3.641 (5.285)	0.356174
57	CD19 B cells among CD66b ⁻ CD45 ⁺	8.33 (3.671)	9.264 (8.883)	0.646487
58	CD20 ⁺ HLADR ⁺ among B cells	2.966 (7.355)	7.78 (20.574)	0.301677
59	CD27 ⁺ CD38 ⁺ plasma cells among CD20 ⁻ HLADR ⁺ B cells	40.636 (23.249)	41.301 (22.297)	0.919915
60	CD20 ⁺ HLADR ⁺ among B cells	95.712 (7.352)	90.113 (22.339)	0.265394
61	CD27 ⁻ IgD ⁺ naïve among CD20 ⁺ HLADR ⁺	66.453 (14.11)	54.928 (20.903)	0.032729
62	CD27 ⁺ IgD ⁻ class-switched memory among CD20 ⁺ HLADR ⁺	13.723 (6.809)	17.912 (9.271)	0.085198
63	CD27 ⁺ IgD ⁺ IgM memory among CD20 ⁺ HLADR ⁺	13.893 (8.827)	17.886 (16.107)	0.303826
64	CD56 ⁻ among CD3 ⁺ CD19 ⁻	89.615 (7.828)	86.881 (6.587)	0.19508
65	TCRgd ⁻ classic T cells among total T cells	97.757 (1.451)	97.493 (1.734)	0.574621
66	CD4 ⁻ CD8 ⁺ among classic T cells	25.705 (9.137)	30.118 (9.619)	0.1116
67	CD45RA ⁻ CCR7 ⁻ TEM among CD8	15.245 (7.516)	13.889 (4.561)	0.446601
68	CD45RA ⁻ CCR7 ⁺ CM among CD8	28.582 (11.591)	19.871 (10.181)	0.007914
69	CD45RA ⁺ CCR7 ⁻ TEMRA among CD8	36.179 (17.486)	49.607 (16.594)	0.008928
70	CD45RA ⁺ CCR7 ⁺ naïve among CD8	17.326 (14.998)	14.272 (11.24)	0.424869
71	CD4 ⁺ CD8 ⁻ among classic T cells	71.145 (9.198)	66.911 (9.867)	0.132923
72	Th1 among CD4 CCR4 ⁻ CXCR5 ⁻	61.282 (16.004)	54.486 (16.115)	0.150608
73	Th2 among CD4 CCR4 ⁺ CXCR5 ⁻	35.101 (11.204)	34.506 (11.046)	0.854118
74	Th17 among CD4 CCR4 ⁺ CXCR5 ⁻	14.757 (7.026)	18.987 (11.054)	0.127509
75	Tfh among CD4 CD45RA ⁻	20.455 (3.61)	18.299 (4.566)	0.079396
76	CD45RA ⁻ CCR7 ⁻ TEM among CD4	12.154 (8.916)	15.618 (5.296)	0.102741
77	CD45RA ⁻ CCR7 ⁺ CM among CD4	47.508 (12.756)	47.847 (9.05)	0.914884

78	CD45RA ⁺ CCR7 ⁻ TEMRA among CD4	4.052 (4.889)	4.934 (5.083)	0.545261
79	CD45RA ⁺ CCR7 ⁺ naïve among CD4	35.278 (16.482)	30.65 (10.146)	0.240098
80	TCRgd ⁺ T among CD56 ⁻	2.24 (1.452)	2.506 (1.736)	0.570601
81	Total NKT among CD56 ⁺	85.402 (12.74)	83.294 (15.719)	0.616183
82	CD8 ⁺ NKT among NKT	59.129 (20.227)	70.188 (16.402)	0.041839
83	CD4 ⁺ NKT among NKT	33.515 (22.057)	20.707 (16.692)	0.026705
84	Eosinophils among CD66b ⁺ CD45 ^{mid}	4.529 (3.466)	2.604 (1.61)	0.014893
85	Neutrophils among CD66b ⁺ CD45 ^{mid}	90.811 (19.671)	97.055 (1.653)	0.114084
86	CD27 ⁺ CD38 ⁺ plasma cells among B cells	0.64 (0.58)	0.91 (1.11)	0.304309
87	CD27 ⁺ IgD ⁺ naïve among B cells	64.28 (15.04)	51.7 (23.15)	0.033506
88	CD27 ⁺ IgD ⁻ class-switched among B cells	12.74 (4.82)	15.03 (8.13)	0.252162
89	CD27 ⁺ IgD ⁺ IgM memory among B cells	13.01 (7.8)	15.6 (15.92)	0.489398

Supplementary Table 6. List of Abs used for the intracellular cytotoxic marker analysis via FCM and/or extracellular Abs for CD8 subset sorting via FACS.

Marker	Fluorochrome	Dilution	Manufacturer	Reference	Clone	Application	Extra-cellular or intra-cellular	Lot number
CD8	BUV496	1/100	BD	612942	RPA-T8	Cytotoxic & Sorting	Extra-cellular	2213972
CD4	BUV395	1/100	BD	563550	SK3	Cytotoxic & Sorting	Extra-cellular	1313997
CD45RA	BV785	1/50	Biolegend	304140	HI100	Cytotoxic & Sorting	Extra-cellular	B369489
CD3	BV510	1/20	BD	564713	HIT3a	Cytotoxic & Sorting	Extra-cellular	2129056
CCR7	BV421	1/50	Biolegend	353208	G043H7	Cytotoxic & Sorting	Extra-cellular	B361376
CD45RO	PE-CF594	1/50	BD	562299	UCHL1	Cytotoxic & Sorting	Extra-cellular	1333677
Perforin	FITC	1/30	Biolegend	353310	B-D48	Cytotoxic	Intra-cellular	B336273
GZMB	RY586	1/750	BD	568133	GB11	Cytotoxic	Intra-cellular	2056267-1
GZMA	Alexa Fluor 700	1/150	Biolegend	507210	CB9	Cytotoxic	Intra-cellular	B322484

GZMK	Alexa Fluor 647	1/30	BD	566655	G3H69	Cytotoxic	Intra- cellular	2234680
------	--------------------	------	----	--------	-------	-----------	--------------------	---------

Of note, for the extracellular and intracellular mastermix, the final volume was 50 μ L and 100 μ L diluted in Brilliant Stain Buffer per reaction, respectively.

Supplementary References

Massena, S., Christoffersson, G., Vågesjö, E., Seignez, C., Gustafsson, K., et al. (2015). "Identification and characterization of VEGF-A–responsive neutrophils expressing CD49d, VEGFR1, and CXCR4 in mice and humans." *Blood* **126**(17): 2016-2026. DOI: 10.1182/blood-2015-03-631572.